Available online at www.sciencedirect.com
SCIENCE DIRECT®
Journal of Nuclear Materials 337–339 (2005) 332–336
journal of nuclear materials
www.elsevier.com/locate/jnucmat

Edge fluctuation studies in Heliotron J

T. Mizuuchi [a,*], V.V. Chechkin [b], K. Ohashi [c], E.L. Sorokovoy [b], A.V. Chechkin [d], V.Yu. Gonchar [d], K. Takahashi [c], S. Kobayashi [a], K. Nagasaki [a], H. Okada [a], S. Yamamoto [a], F. Sano [a], K. Kondo [c], N. Nishino [e], H. Kawazome [c], H. Shidara [c], S. Kaneko [c], Y. Fukagawa [c], Y. Morita [c], S. Nakazawa [c], S. Nishio [c], S. Tsuboi [c], M. Yamada [c]

[a] *Institute of Advanced Energy, Kyoto University, Gokasho, Uji 611-0011, Japan*
[b] *Institute of Plasma Physics, NSC KIPT, 61108 Kharkov, Ukraine*
[c] *Graduate School of Energy Science, Kyoto University, Gokasho, Uji 611-0011, Japan*
[d] *Institute for Theoretical Physics, NSC KIPT, 61108 Kharkov, Ukraine*
[e] *Graduate School of Engineering, Hiroshima University, Hiroshima 739-8527, Japan*

Abstract

Low frequency and small-scale fluctuations of density and potential near the last closed flux surface are investigated by using Langmuir probes for the second harmonic ECH plasmas in a helical-axis heliotron device, Heliotron J. The existence of a plasma layer with a radial electric field shear was indicated near the last closed flux surface. Near this layer, the reversal of phase velocity and de-correlation of the fluctuations were observed. On the other hand, it is suggested that a considerable fraction of the fluctuation induced particle flux is carried off through the intermittent events. Preliminary analyses to classify the PDFs of the ion-saturation current fluctuation as stable Lévy distributions demonstrate that the Lévy index decreases from the inner to the outer region of edge plasma, suggesting that the PDFs near the boundary region of Heliotron J are nearly Gaussian, whereas at the outer regions of plasma they become strongly non-Gaussian.

PACS: 52.55.Hc; 05.40.+j; 52.35.Oz
Keywords: Heliotron J; Edge-plasma; Fluctuation and turbulence; Intermittent transport

1. Introduction

The fluctuation of density and potential in the edge plasma is considered to play a key role in the anomalous transport in various types of magnetic confinement devices [1]. Recent experiments in different devices demonstrate that the profile of radial electric field $\boldsymbol{E}_r$ near the plasma edge strongly affects the fluctuation; the $\boldsymbol{E}_r$-shear can suppress the correlation between the density and potential fluctuations [2]. On the other hand, the edge fluctuations observed in many devices are characterized by the appearance of sharp spikes with large amplitude (intermittent events) [3]. It is possible that these intermittent events play a significant role in the edge plasma

* Corresponding author. Tel.: +81 774 38 3451; fax: +81 774 38 3535.
E-mail address: mizuuchi@iae.kyoto-u.ac.jp (T. Mizuuchi).

0022-3115/$ - see front matter © 2004 Elsevier B.V. All rights reserved.
doi:10.1016/j.jnucmat.2004.10.010

transport crossing the magnetic field to the first wall [4]. In order to understand such intermittent events, many theorists and experimentalists pay much attention to the statistical analysis of the turbulence based on non-Gaussian random processes [5,6].

This paper reports initial results from the experimental studies of edge plasma fluctuation observed in Heliotron J ECH plasmas.

2. Experiments

The details of Heliotron J, a medium sized $L = 1/M = 4$ helical-axis heliotron device, are described elsewhere [7,8]. To study low frequency (1–200 kHz) and small-scale ($k_\perp \sim 1$–$2\ \mathrm{cm}^{-1}$) fluctuations of density (ion saturation current, I_s) and potential (floating potential, V_f) near the last closed flux surface (LCFS), we used three Langmuir probes, which were a part of a poloidal probe array with 17 pins (#9–#11 probes of the array) [9]. The probe pins were aligned nearly parallel to the shape of the calculated LCFS in one poloidal cross-section of the torus. The distance between adjacent probes (molybdenum probe tips of 1.5 mm in diameter × 2 mm in length) was 5 mm. The ion-saturation current was measured by #9-probe and the other two probes monitored floating potentials, V_{f10} and V_{f11}. Second harmonic ECH plasmas ($f_{ECH} = 70$ GHz, $P_{ECH}^{inj.} \sim 240$–310 kW, $B = 1.25$ T) with $\bar{n}_e \sim (0.4$–$1.0) \times 10^{19}\ \mathrm{m}^{-3}$ were investigated under two magnetic field configurations, a 'high bumpiness' configuration (HBC, the edge rotational transform $\iota(a)/2\pi \approx 0.55$) and the 'standard' configuration (STD, $\iota(a)/2\pi \approx 0.56$). The calculated LCFS positions (without plasma) for the HBC and STD cases are $R_0 \approx 136.3$ cm and 136.6 cm, respectively, for #10-probe. On the outside the LCFS, the radial profile of the 'D.C.' component of the ion-saturation current, $\overline{I}_s$, shows a monotonic decay with the characteristic lengths of ~2 cm (HBC) and ~3 cm (STD). The values of the 'D.C.' component of the floating potential, $\overline{V}_f$, measured by the #10 and #11 probes were almost the same for all values of R in the HBC case. In the STD case, however, it was observed a large difference between $\overline{V}_{f10}$ and $\overline{V}_{f11}$. The reason of this potential difference is under investigation. The detailed comparison of plasma performance between these two configurations is in progress and will be reported elsewhere.

3. Characteristics of edge fluctuations

3.1. Radial dependence of edge fluctuation properties

Fig. 1 shows time traces of the core density (the line integrated density along the center chord), $n_e l$, the plasma stored energy (the diamagnetic-loop signal), W_p, Hα-signal, Hα, and the ion-saturation current, I_s, for a typical ECH discharge in the HBC configuration. As shown in the insertion of Fig. 1, the fluctuations include bursting spikes.

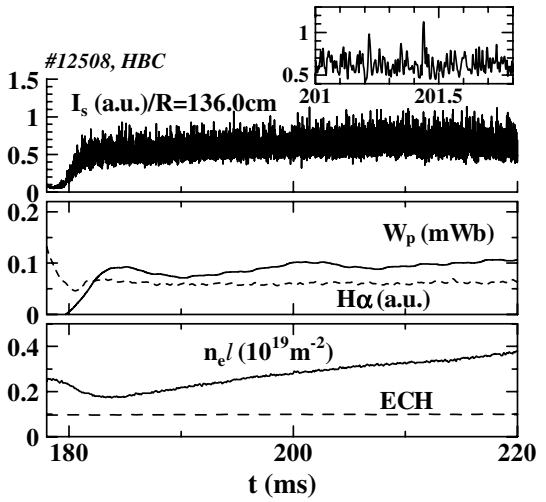

Fig. 1. Typical time traces of the core density, $n_e l$, the diamagnetic-loop signal, W_p, Hα-signal, Hα, and the ion-saturation current, I_s for ECH discharges in the HBC configuration.

In the HBC configuration, the radial scan of the probes under the fixed condition of $\bar{n}_e \approx 1 \times 10^{19}\ \mathrm{m}^{-3}$ revealed that the frequency dependence of the fluctuation power spectra depends on the radial positions, R, as shown in Fig. 2, where the power spectra of $\widetilde{I}_s$ are plotted for three different positions. Inside the LCFS, the power spectra are broad. Then it becomes clearly narrower as the probe moves within the range of 136.2 cm < R < 137.2 cm and broadens again with further drawing out the probe from the boundary.

For the same discharge set as in Fig. 2, the radial profile of $\overline{V}_f$ is plotted in Fig. 3. As inserting the probes toward the LCFS, the potential $\overline{V}_f(R)$ increases and it has a positive maximum at $R \approx 137$ cm. Then it starts to decrease and becomes negative at $R < R_0$ Since the change of electron temperature (estimated from the probe I–V characteristic) was not so large near the LCFS, the plasma potential as a function of R is considered to have qualitatively the same form as $\overline{V}_f(R)$. Thus, near the boundary of the confinement region, a plasma layer is formed where the radial electric field $\boldsymbol{E}_r$ reverses its direction ($\boldsymbol{E}_r$ is directed inward at $R < 137$ cm and outward at $R > 137$ cm), indicating that a shear of the velocity of the 'equilibrium' $\boldsymbol{E} \times \boldsymbol{B}$ rotation of the plasma should be produced near this layer. According to Fig. 3, $E_r \sim -3 \times 10^3$ V/m is estimated near the LCFS. The corresponding plasma poloidal rotation velocity is

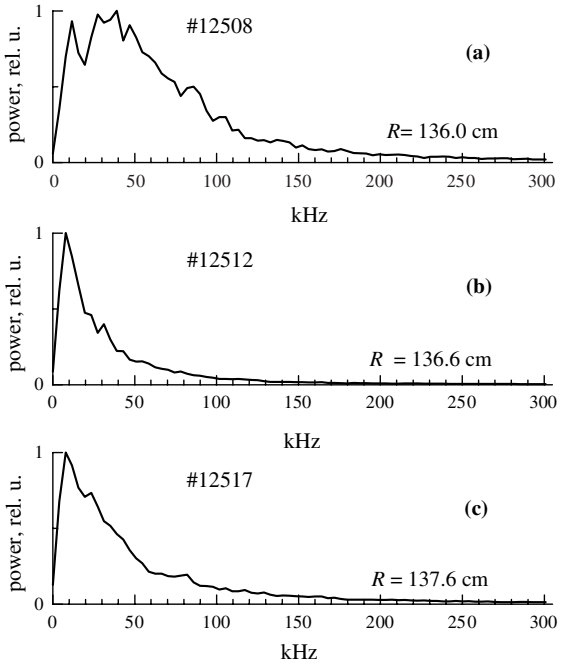

Fig. 2. Normalized power spectra of I_s for three positions (HBC).

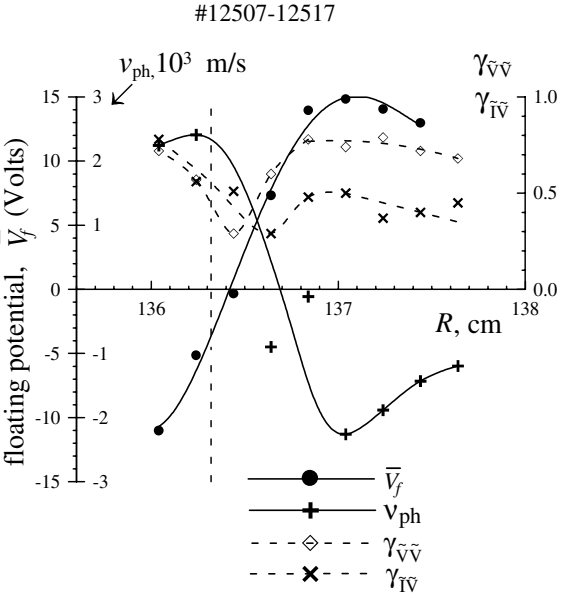

Fig. 3. Radial dependences of the floating potential V_f (V_{f10}), the averaged phase velocity v_{ph} and the coherence between V_{f10} and V_{f11} at 30 kHz, $\gamma_{\tilde{V}\tilde{V}}$, and the coherence between I_s and V_{f10} at 30 kHz, $\gamma_{\tilde{I}\tilde{V}}$. The vertical dashed line indicates the position of LCFS for #10-probe (HBC).

$|V_{E\times B}| \sim 2\times 10^3$ m/s in the direction of the electron diamagnetic drift.

It is expected that edge turbulence characteristics are affected by this velocity shear, resulting in reversal of propagation of the fluctuations due to the $\boldsymbol{E}_r \times \boldsymbol{B}$ 'Doppler shift' and in their de-correlation [2]. In the frequency range of 5–100 kHz, where the maximum fluctuation intensity falls, the direction of the *average phase velocity* along the line of probe alignment, v_{ph}, can be determined and the value of v_{ph} can be estimated by the slope of the trend of the fluctuation cross-phase spectra between V_{f10} and V_{f11} (Fig. 3). Inside the LCFS (R = 136.3 cm), the direction of v_{ph} corresponds to the direction of the electron diamagnetic drift, and $|v_{ph}|$ is 2.3×10^3 m/s, which is the same order as $|V_{E\times B}|$ mentioned above. As shown in Fig. 3, v_{ph} reverses its direction near the $\boldsymbol{E}_r$-shear layer. These observations suggest that the propagation of the turbulence is dominated by the equilibrium plasma rotation probably caused by $\boldsymbol{E}_r \times \boldsymbol{B}$.

The shear of plasma rotation velocity is expected to suppress the correlation between the fluctuations of plasma density and potential near this layer. The coherence between $\tilde{I}_s$ and $\tilde{V}_f$ at 30 kHz, $\gamma_{\tilde{I}\tilde{V}}$, is plotted in Fig. 3 as a way of example. It is seen that $\gamma_{\tilde{I}\tilde{V}}$ drops in the vicinity of the $\boldsymbol{E}_r \times \boldsymbol{B}$ shear-layer from a rather high (~0.6–0.7 at R = 136.0 cm and R = 136.6 cm) to a low value (~0.4 at R = 136.6 cm). Also, the coherence between the floating potential oscillations, $\gamma_{\tilde{V}\tilde{V}}$, behaves similarly, taking the values of ~0.68 and ~0.79 at R = 136 cm and R = 136.8 cm, respectively, and falling to ~0.31 at an intermediate position R = 136.4 cm.

The similar properties of edge plasma potential and fluctuation were observed also in the STD case. In contrast to the HBC case, however, a complete $\boldsymbol{E}_r$ shear layer seems not to occur at lower-density plasmas for the STD case. This density dependence on the fluctuation behavior might be related to the critical density ($\bar{n}_e > 1.2\times 10^{19}$ m^{-3}) for the H-mode transition observed in Heliotron J [10]. The experiments from this point of view will be performed soon.

3.2. Time behavior of turbulent particle flux

Since the three probes used in this study are aligned poloidally and parallel to the LCFS, a qualitative character of time variation of the fluctuation-induced radial particle flux, $\tilde{\Gamma}(t) = \tilde{n}(t)\tilde{v}(t) \propto \tilde{n}(t)\tilde{E}_p(t)/B_t$ can be discussed by considering a function of experimental values $\tilde{G}(t) = \tilde{I}_s(t)(\tilde{V}_{f10}(t) - \tilde{V}_{f11}(t))$, assuming $\tilde{n}(t) \propto \tilde{I}_s(t)$, the poloidal electric field $\tilde{E}_p(t) \propto \tilde{V}_{f10}(t) - \tilde{V}_{f11}(t)$ and B_t = constant, similar to what has been done in [3]. As an example, $\tilde{G}(t)$ at R = 137.6 cm for an ECH discharge with the $\bar{n}_e \approx 9\times 10^{18}$ m^{-3} in the STD configuration is shown in Fig. 4(a). It is seen that the flux is predominantly positive, i.e., directed outwards. It is also shown that a considerable fraction of the flux is carried by large random 'bursts', whose amplitudes multiply exceed the average flux G. In Fig. 4(b), the radial dependences are

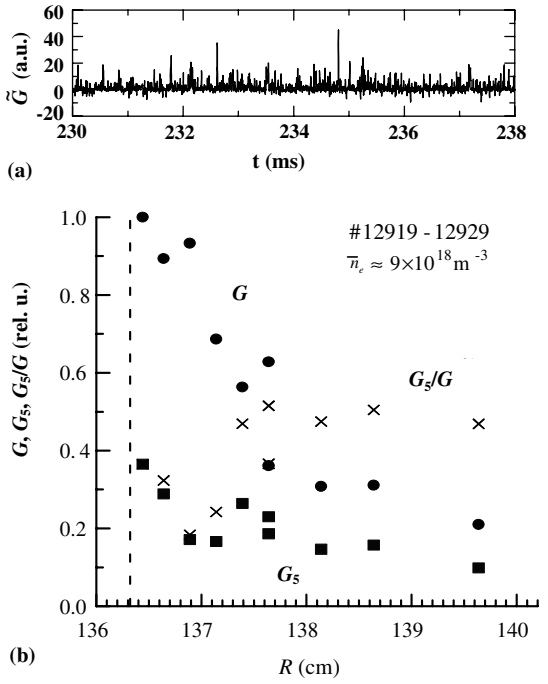

Fig. 4. Time behavior of function $\widetilde{G}(t)$ at $R = 137.6$ cm. Time-integrated function of $\widetilde{G}(t)$, designated as G (●), and its fraction G_5 (■) containing the bursts with a fivefold and more excess of their amplitude over the average versus major radius R. ($\bar{n}_e \approx \times10^{18}$ m^{-3}, STD). The ratio of G_5/G is also plotted by (×). The vertical dashed line indicates the position of LCFS for #10-probe.

shown of the time-integrated function, designated as G, that is proportional to the total time-integrated turbulent flux, and of its fraction G_5 including the bursts with a fivefold and more excess of their amplitude over the average $\widetilde{G}$ level. Both quantities, G and G_5, decay with distance from the LCFS. However, it is interesting to note that their ratio ($\geqslant 0.4$) does not change substantially in the outer region.

4. Statistical properties of edge plasma fluctuations

Density and potential fluctuations in the edge plasma are characterized by the appearance of sharp spikes with large amplitude also in Heliotron J. Such behavior of random signals is considered as a result of the intermittency of plasma turbulence. Because of the presence of spikes, the probability distribution function (PDF) of fluctuation magnitude can be different from a Gaussian distribution. The kurtosis, the fourth moment of the PDF, is often used as a measure of the intermittency. However, more detailed information on PDFs is necessary to assign the observed distribution to a particular class of the probability laws widely used in various

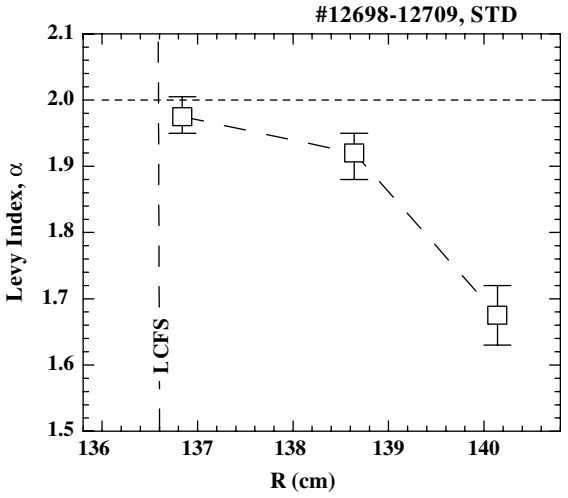

Fig. 5. Radial dependence of Lévy index α for I_s (STD).

applications. Stable Lévy distributions are useful for mathematical models for non-Gaussian random processes. These distributions can be classified by so-called Lévy index, α, varying from $\alpha = 0$ to 2. Here, $\alpha = 2$ corresponds to the Gaussian distribution. From this point of view, we have tried to evaluate the parameters of stable distributions for the fluctuations observed in Heliotron J by using the analyzing method discussed in [6].

As a preliminarily analysis, the Lévy index for the fluctuation of the ion-saturation current was evaluated by using 72 000 points of data ($t = 202$–274 ms). The estimated Lévy index is shown in Fig. 5 for the three radial positions. As shown in the figure, α for $\widetilde{I}_s$ decreases with distance from the plasma boundary, indicating the distribution asymptotics become flatter, and spikes in the experimental samples become more distinct. At $R = 136.8$ cm, the index α (with allowance for the error bars) is close to 2 (Gaussian PDF). However, the PDF deviates from Gaussian at large radii, and the deviation seems to increase with R.

The same tendency was observed previously in fluctuations measured in Uragan 3-M [6]. At present, we have no definite answer why the Lévy index decreases from the inner to the outer region of plasma. More detailed analytical and numerical analysis based on many experimental data is necessary. Moreover, it is interesting to examine the properties of PDFs for the fluctuation induced particle flux.

5. Summary

Characteristics of low frequency and small-scale fluctuations of density and potential near the LCFS are studied by using Langmuir probes for the second harmonic ECH plasmas in Heliotron J.

It was observed that a plasma layer with $\boldsymbol{E}_r$ shear is formed near the boundary of the confinement region. The reversal of propagation and de-correlation of the fluctuations were observed near this layer. The narrowing of the spectrum band in the fluctuation power spectra was also observed near this layer.

The time behavior of the fluctuation induced particle flux is examined based on the probe data. It is shown that the flux is predominantly directed outward and a considerable fraction of the flux is carried by large 'bursts', whose amplitudes multiply exceed the average flux.

Preliminary analyses to classify the PDFs of the observed fluctuations as stable Lévy distributions were performed. Moving from the inner to the outer region of edge plasma, the Lévy index decreases, suggesting that the PDFs of the turbulence near the boundary region of Heliotron J are nearly Gaussian, whereas at the outer regions of plasma they become strongly non-Gaussian.

Acknowledgments

The authors thanks to the technical staff of the Heliotron J team for their excellent assistance in the experiments. This research was partially supported by LIME Program of MEXT in Japan and the Collaboration Program of the Laboratory for Complex Energy Processes, IAE, Kyoto University.

References

[1] M. Endler, J. Nucl. Mater. 266–269 (1999) 84.
[2] K.H. Burrell, Phys. Plasmas 4 (1997) 1499.
[3] B.A. Carreras, C. Hidalgo, E. Sanches, et al., Phys. Plasmas 3 (1996) 2664.
[4] G.Q. Yu, S.I. Krasheninnikov, Phys. Plasmas 10 (2003) 4413.
[5] R. Jha, P.K. Kaw, D.R. Kulkarni, J.C. Parikh, Phys. Plasmas 3 (2003) 699.
[6] V.Yu. Gonchar, A.V. Chechkin, E.L. Sorokovoy, et al., Plasma Phys. Rep. 29 (2003) 380.
[7] T. Obiki, T. Mizuuchi, K. Nagasaki, et al., Nucl. Fusion 41 (2001) 833.
[8] T. Obiki, T. Mizuuchi, H. Okada, et al., Nucl. Fusion 44 (2004) 47.
[9] T. Mizuuchi, W.L. Ang, Y. Nishioka, et al., J. Nucl. Mater. 313–316 (2003) 947.
[10] F. Sano, T. Mizuuchi, K. Nagasaki, et al., J. Plasma Fusion Res. 79 (2003) 1111.